frontiers | Frontiers in Earth Science

TYPE Original Research
PUBLISHED 29 September 2022
DOI 10.3389/feart.2022.1032018

Check for updates

OPEN ACCESS

EDITED BY
Shu Jiang,
The University of Utah, United States

REVIEWED BY
Xin Li,
China National Offshore Oil Corporation, China
Anna Davis,
Chevron, United States
Tingwei Li,
Guangzhou Marine Geological Survey, China

*CORRESPONDENCE
Kun Zhang,
shandongzhangkun@126.com

SPECIALTY SECTION
This article was submitted to Economic Geology,
a section of the journal
Frontiers in Earth Science

RECEIVED 30 August 2022
ACCEPTED 12 September 2022
PUBLISHED 29 September 2022

CITATION
Yuan X, Zhang K, Peng J, Li B, Han F, Chen X, Zheng Z, Ruan J, Ye L, Wang Z, Huang Z, Chen K, Wu M, Niu J and Yang Z (2022), Study on characteristics of oil and gas occurrence and reservoir space of medium-high maturity continental shale—A case study of middle jurassic lianggaoshan formation in fuling block, southeast of sichuan basin, south China.
Front. Earth Sci. 10:1032018.
doi: 10.3389/feart.2022.1032018

Study on characteristics of oil and gas occurrence and reservoir space of medium-high maturity continental shale—A case study of middle jurassic lianggaoshan formation in fuling block, southeast of sichuan basin, south China

Xuejiao Yuan[1,2], Kun Zhang[1,2,3,4]*, Jun Peng[1,2], Bin Li[1,2], Fengli Han[1,2], Xuecheng Chen[1,2], Zehao Zheng[1,2], Jingru Ruan[1,2], Laiting Ye[1,2], Zeyun Wang[1,2], Zhen Huang[1,2], Kun Chen[1,2], Meijia Wu[1,2], Jiale Niu[1,2] and Zhendong Yang[1,2]

[1]School of Geoscience and Technology, Southwest Petroleum University, Chengdu, China, [2]Natural Gas Geology Key Laboratory of Sichuan Province, Southwest Petroleum University, Chengdu, China, [3]Key Laboratory of Tectonics and Petroleum Resources (China University of Geosciences), Ministry of Education, Wuhan, China, [4]Energy and Geoscience Institute, University of Utah, Salt Lake City, UT, United States

Possessed of easy access to development and fair economic benefits, medium-high maturity continental shale oil and gas have become the focus of shale oil and gas study in the future. Shale oil and gas mainly occur in pores, but studies on the pore characteristics of shale oil and gas occurrence are by no means sufficient. Focused on shale from the Middle Jurassic Lianggaoshan Formation in Well TYX, Fuling block, southeast of Sichuan Basin where a breakthrough in shale oil and gas exploration was recently achieved, this study selects core samples and conducts a series of analyses, including vitrinite reflectance analysis, kerogen microscopic examination experiment, total organic carbon (TOC) content analysis, mineral composition analysis, gas content measurement, isothermal adsorption experiment, S_1 content analysis, and others. The analyses are to identify the pore characteristics of the continental medium and high maturity shale oil and gas by virtue of scanning electron microscope (SEM) with Ar-ion milling and the image processing software ImageJ. The conclusions are drawn as follows: in terms of lithofacies, medium-high maturity continental shale oil and gas mainly occur in organic-rich clay shale and organic-rich mixed shale; with regard to material composition, shale oil and gas mainly occur in organic matter, illite-smectite mixed layers and illite. Shale adsorbed gas content accounts for at most 40% of the total shale gas content and shale free gas content takes up at least 60% of the total shale gas content. Pores of solid bitumen, solid bitumen-clay mineral complex mass, clay minerals, structured vitrinite, and funginite are mostly developed in shale. Among them, the first three types of pores are the main reservoir space in shale considering their large number, good roundness, medium pore diameter, fairly good roundness of pore edges, and the complex shapes which altogether contribute to the large surface porosity.

KEYWORDS

continental shale oil and gas, medium-high maturity shale, occurrence and reservoir space, lithofacies type, material composition, pore type

Introduction

Thanks to the geological theory of shale oil and gas and the advancement of horizontal well drilling technology and fracking technology, marine shale oil and gas have managed to be commercially explored and developed on a large scale in North America in recent years (Bazilian et al., 2014; Loucks et al., 2017; Adeleye and Akanji, 2018; Ardakani et al., 2018; Bakshi and Vishal, 2021). China also boasts huge shale oil and gas resources of marine, continental and marine-continental transitional facies. Since 2010, China National Petroleum Corporation (CNPC) and China Petroleum & Chemical Corporation (Sinopec Corp) have obtained commercial breakthroughs in marine shale gas of the Lower Silurian Longmaxi Formation in blocks like Weiyuan, Changning, Jiaoshiba, Weirong, Luzhou, Zhaotong, Yongchuan, Dingshan, et al. (Guo, 2016; Li et al., 2019; Nie et al., 2019; Wang et al., 2019; Fan et al., 2022). In addition to shale gas, China is also practicing the exploration and development of shale oil. In continental strata, when the organic matter in shale is at medium-high maturity (maturity Ro>0.9%), shale oil is light (relative density<0.87), which makes it easy to be exploited in light of its great mobility. In this way, the economic benefits are considerable, and accordingly light shale oil has become the key research object at present. (Zhang et al., 2019b; Liu B. et al., 2021; Liu et al., 2021c).

The characteristics of shale oil and gas occurrence and reservoir space figure prominently in the study of shale reservoir characteristics (He et al., 2019; He et al., 2020). Previous studies have been carried out on the characteristics of shale reservoirs (Gao et al., 2018; Jin et al., 2018; Gao et al., 2020; Jin et al., 2020; Li, 2022). To be specific, by virtue of rock thin section, SEM with Ar-ion milling, nuclear magnetic resonance (NMR), high-pressure mercury intrusion and low-temperature nitrogen adsorption experiment, a study was conducted on the low maturity continental shale strata of Lower Sub-member 3-Upper Sub-member 4 in Paleogene Shahejie Formation, Dongying Sag. Data about pore structure and porosity of shale reservoirs were obtained, and analyses of the influences that mineral composition and organic matter content exerted on porosity and pore diameter were also conducted. The above data and analysis results were further combined to form thermal simulation experiments where the evolutionary characteristics of main pore types were discussed Zhang et al. (2018). Taking advantage of SEM, Soxhlet extractor method, gas adsorption, NMR (including centrifugation) and other methods, a study was carried out on the muddy shale in the lower sub-member of the Member 3 of Shahejie Formation in Zhanhua Sag in order to ascertain the influences of reservoir characteristics of muddy shale on the mobility of shale oil, and to understand its mechanism of action (MOA) Jiang et al. (2020). In view of the diverse types of shale oil reservoirs and great difficulty in sweet-spot prediction in the Lucaogou Formation, analysis on the mechanism influencing shale oil pore development and evaluation on oil-bearing properties, are supposed to be carried out. To this end, this study focuses on the microscopic pore structure of shale oil reservoirs in the Permian Lucaogou Formation, Jimsar Sag, through an integration of core observation, SEM, mercury intrusion porosimetry (MIP) and NMR, etc. As a result, the influential mechanism is disclosed and classification criteria for reservoir evaluation are set up Wang L et al. (2022).

Although systemic studies have been carried out on the reservoir characteristics of shale, research on the characteristics of oil and gas occurrence and reservoir space of medium-high maturity continental shale is still insufficient. With Well TYX as a research object in the Fuling block, southeast of Sichuan Basin where a commercial breakthrough in continental light shale oil was recently made, this study proceeds in the following order: first the gas content and oil content of shale of different lithofacies types are analyzed; second the reservoir space where shale oil and gas occur is identified; third the main pore types of shale is recognized by virtue of SEM, and the SEM image is analyzed using the image processing software ImageJ, so that the pore characteristics of shale of different matrices are quantitatively characterized; finally the patterns of pore characteristics of shale oil and gas occurrence are summarized.

Geological settings

Sedimentary and stratum characteristics

The Middle Jurassic Sichuan Basin was a depression basin, and the block located in the southeast of the Sichuan Basin which is under investigation in this study experienced a complete transgression-regression cycle during the sedimentary period of the Lianggaoshan Formation. (Gao et al., 2017; Li et al., 2020c; Liu et al., 2020; Gao, 2021; Wang Z et al., 2022). From bottom to top, the Lianggaoshan Formation can be divided into 3 members and they are Member I, Member II and Member III. Moreover, Member I and Member II can be further subdivided into upper and lower submembers, respectively. Among them, the upper submember of Member I and the lower submember of Member II were shallow to semi-deep lake depositional environments. In other words, the submembers are organic-rich shale, as well as shale oil and gas enrichment strata.

Tectonic characteristics

As is shown in Figure 1, the block is located in the high-angle fault fold belt in the southeastern Sichuan Basin. The west of the high-angle fault fold belt is bounded by the Huayingshan fault and is adjacent to Chuanzhong Uplift, and the east of the belt, reaching up to the Qiyueshan fault zone, is made up of a series of arc-shaped mountains (Li et al., 2010; Liu and Ni, 2010; Pang et al., 2019; Qing et al., 2019; Li et al., 2020b). The arc-shaped mountain range is a high-angle anticline with the Permian-Triassic as the core. The two wings of the range are asymmetrical. Generally, the dip angle of the stratum on the gentle wing is 20°–30°, and that on the steep wing is 40°–70° and the stratum can even be upright and inverted. (Li et al., 2017; Li H. et al., 2020; Li et al., 2021a; Li et al., 2022a). The broad valleys between the arc-shaped mountains are Jurassic trapped syncline. The high-angle fault fold belt is ejective from both tectonic and geomorphic aspects (Wang et al., 2018; Wang et al., 2021a; Li et al., 2021b; Wang et al., 2021b).

Samples, experiments, and data sources

Organic matter maturity, TOC content analysis, mineral composition analysis

In this study, a uniform sampling was conducted on the shale from the shale core section of the Lianggaoshan Formation in Well TYX and the specific sampling depth is shown in Figure 2. Specifically, 7 samples were selected to carry out organic matter vitrinite reflectance analysis and the organic matter vitrinite reflectance analyzers of ZEISS Imger A2m and J&M MSP200 were utilized to analyze the shale organic matter maturity; 205 samples were selected to perform TOC content analysis and the TOC content analyzer of Sievers 860 were used; 72 samples were selected to do mineral composition analysis and the mineral analyzer of YST-I was used to conduct X-ray diffraction whole rock mineral analysis.

Rock pyrolysis experiment

Rock pyrolysis, put forward by the French Institute of Petroleum (IFP), can evaluate source rocks in a short time period. The basic principle is to pyrolyze source rocks by heating the rock samples in certain instruments and afterwards the source rocks are evaluated on the basis of the type and quantity of products. The pyrolysis results are displayed in the pyrolysis spectrum which has three peaks. Particularly, the P_1 peak turns up when pyrolysis temperature is less than 300°C, and the area of the peak is represented by S_1. The residual hydrocarbon content in the rock is displayed by kg (hydrocarbon)/t (rock), which is equivalent to chloroform bitumen “A”. This study conducted a uniform sampling and 38 samples were selected form the shale core section of Lianggaoshan Formation in Well TYX, and the specific sampling depth is shown in Figure 2. An instrument of ROCK Eval 7 was utilized to perform the rock pyrolysis experiment.

On-site analysis of total gas content in shale

The total gas content of shale plays an important role in evaluating the oil-gas-bearing potential of shale. The shale gas analyzer can measure the residual shale gas content at the core of shale in the well sites, and the original total gas content of shale can be simulated by mathematical formula. This study conducted a closed sampling and 70 samples were selected from the core section of the Lianggaoshan Formation in Well TYX, and the specific sampling depth is shown in Figure 2. An analytical gas analyzer of YSQ-IV was used to measure the total gas content of shale.

Isothermal adsorption experiment

The isothermal adsorption experiment can quantitatively analyze the maximum adsorption capacity of shale. In this study, 10 samples were selected from the core section of Lianggaoshan Formation in Well TYX, which are shown in Figure 2. The isothermal adsorption apparatus of FY-KT 1000 was used to conduct the experiment at a temperature of 125°C.

FIB-SEM observation

Focused ion beam scanning electron microscope (FIB-SEM) can perfectly identify the microscopic mineral composition and pore type of shale. FIB technology is a new technique with high resolution that focuses the ion beam spot to sub-micron or even

10.3389/feart.2022.1032018

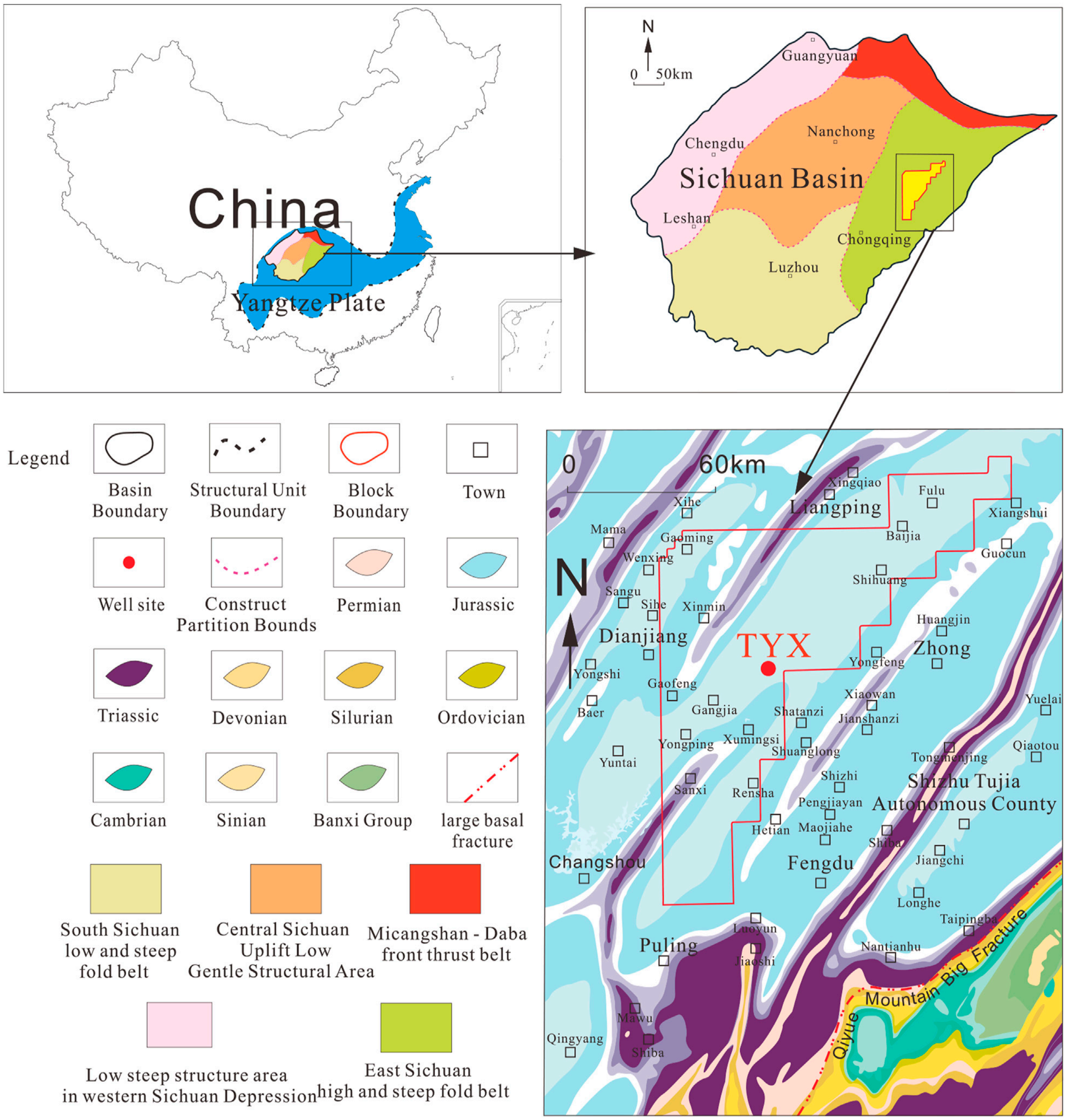

FIGURE 1
Location of the Fuling block and the distribution of TYX well sites in the southeast of Sichuan Basin, South China. Modified from references (Guo et al., 2016; Guo et al., 2017; Liu W. et al., 2021; Wei et al., 2021; Zhang et al., 2022b).

nanometre scale and realizes microfabrication with a deflection system. A FIB-SEM sample can only be obtained through several procedures, such as grinding, Ar-ion milling, carbon spraying, etc. The rather mature secondary electron imaging technology of FIB-SEM can fairly identify the surface topography of minerals and pores, in particular. With this technology in use, the micro-nanometre pores of shale are bright all around, which makes it easy to be identified and together with the backscattered

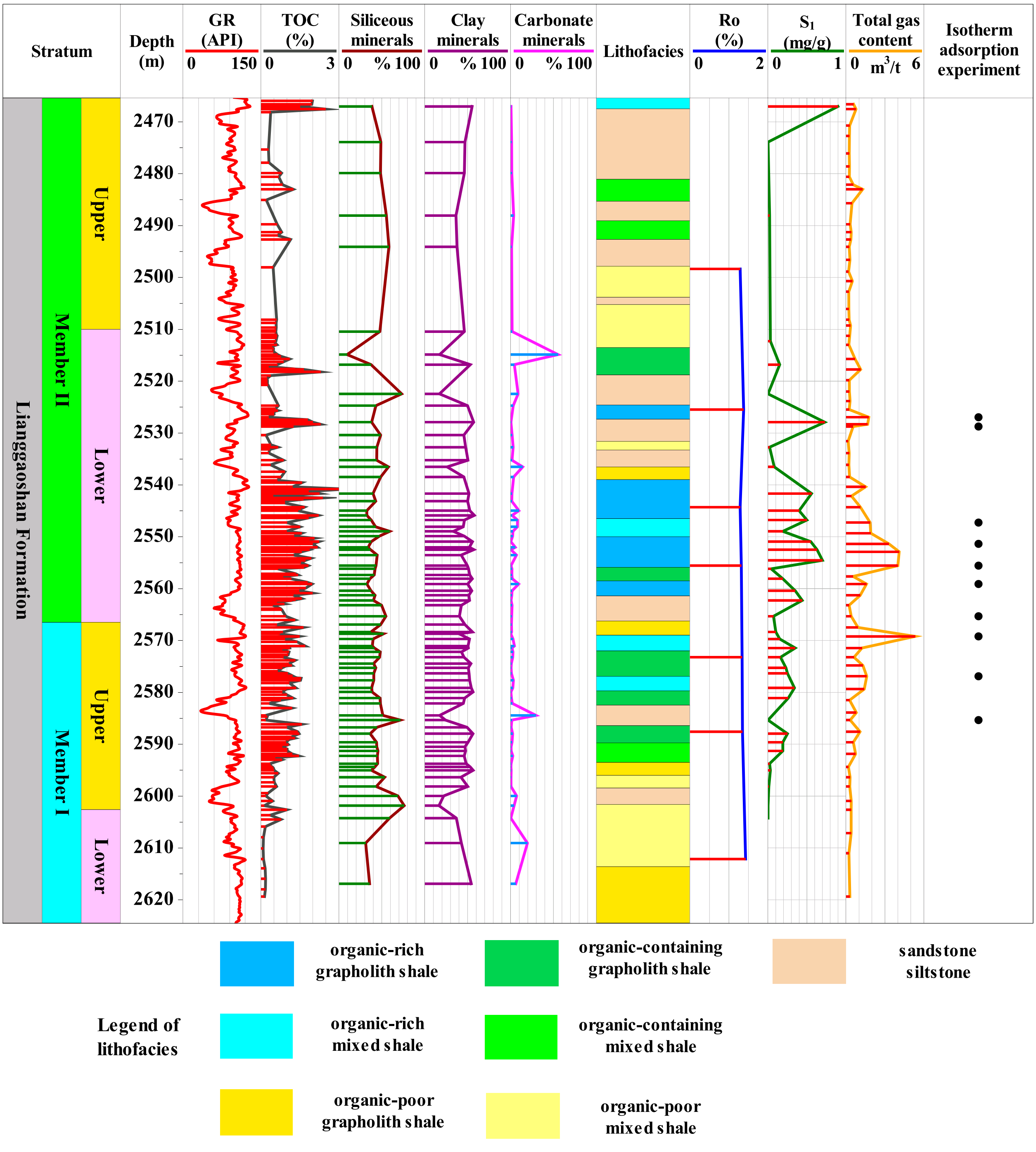

FIGURE 2
Comprehensie histogram of sampling depth, analysis and test results of the samples, and lithofacies division results in Member I and Member II of Well TYX. Modified from references (Liu W. et al., 2021; Wei et al., 2021; Zhang et al., 2022b). See Figure 1 for the well location.

technology of FIB-SEM which can help identify the mineral composition, the type of shale micro-nanometre pores can be effectively determined (Zhang et al., 2019c; Li et al., 2021c; Zhang et al., 2022d; Zhang et al., 2022e). In this study, FIB-SEM observation was carried out using an instrument of FEI HELIOS NANOLAB 650 SEM.

Results and discussion

Analysis of shale organic matter maturity

The analysis results of shale organic matter maturity are shown in the table below. According to Table 1, it can be seen that Ro of organic matter of Lianggaoshan Formation shale in Well TYX ranges from 1.29 to 1.38%, with an average value of 1.34%.

China's continental shale oil resources are generally divided into two categories according to their maturity. When Ro is greater than 0.9%, the shale oil is believed to have medium-high maturity, and when the situation is opposite, it is called medium-low maturity shale oil. The shale oil of Lianggaoshan Formation in Well TYX is of medium-high maturity. When Ro is greater than 0.9%, the original organic matter (kerogen) evolves into a massive hydrocarbon generation stage, and the occluded hydrocarbons (petroleum, bitumen, etc.) fill the organic and inorganic pores of shale.

Lithofacies division of shale

The division schemes of shale lithofacies were proposed based on TOC content and mineral composition in previous studies: 1) according to TOC content, shale was divided into 3 types and they are: organic-rich shale (TOC content:≥2%), organic-bearing shale (TOC content: 1–2%), and organic-lean shale (TOC content: 0–1%); 2) according to mineral composition, shale was divided into 4 types and they are: calcareous shale (carbonate minerals ≥50%), clayey shale (clay minerals ≥50%), siliceous shale (siliceous minerals ≥50%), mixed shale (siliceous minerals, clay minerals and carbonate minerals are all less than 50%) (Clarkson et al., 2013; Daigle et al., 2017; Zhang et al., 2019a; Li et al., 2022b; Zhang et al., 2022c). In combination with the two division schemes, there appear 3×4=12 types of lithofacies. Based on the TOC content and mineral composition of shale samples, the shale lithofacies are divided as shown in the figure.

TABLE 1 Analysis results of organic matter maturity of Lianggaoshan Formation shale in Well TYX.

Stratum	Depth	Ro (%)
Upper submember of Member II	2498.37	1.29
Lower submember of Member II	2525.47	1.38
Lower submember of Member II	2544.28	1.29
Lower submember of Member II	2555.56	1.32
Upper submember of Member I	2573.23	1.34
Upper submember of Member I	2587.58	1.35
Lower submember of Member I	2612.12	1.43

Analysis of S_1 content in shale of different lithofacies types

The analysis results of S_1 content in shale are shown in Figure 2. The statistical analysis of S_1 content in shale of different lithofacies types is shown in Figure 3, according to which, S_1 content in organic-rich clayey shale is the highest, with an average value of 0.58 mg/g; S_1 content in organic-rich mixed shale is the second highest, with an average value of 0.41 mg/g; S_1 content in organic-bearing clayey shale, as well as organic-bearing mixed shale, is around 0.19 mg/g; S_1 content in organic-lean clayey shale, organic-lean mixed shale and sandstone is as low as 0.01–0.05 mg/g.

Analysis of gas content in shale of different lithofacies types

Analysis of total gas content in shale

The analysis results of gas content in shale are shown in Figure 2 and the statistical analysis of gas content in shale of different lithofacies types is shown in Figure 4. According to Figure 4, gas content in organic-rich mixed shale is the highest, with an average value of 2.59 m^3/t; gas content in organic-rich clayey shale is the second highest, with an average value of 1.68 m^3/t; gas content in organic-bearing clayey shale and organic-bearing mixed shale is around 1.58–1.13 m^3/t; gas content in organic-lean clayey shale, organic-lean mixed shale and sandstone is the lowest, that is, 0.35–0.51 m^3/t.

Analysis of adsorbed gas content and free gas content

The Langmuir volume and Langmuir pressure of each shale sample can be obtained through the isotherm adsorption

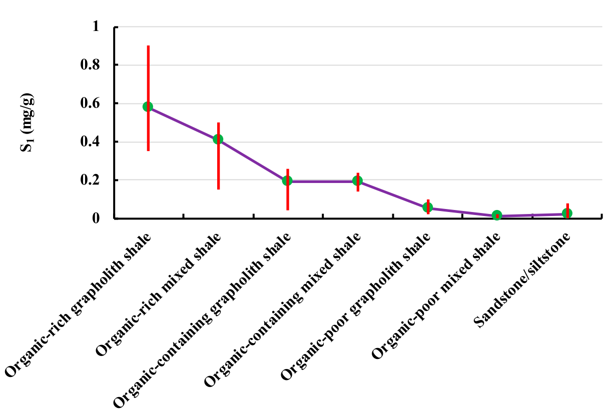

FIGURE 3
Characteristics of S_1 content in shale of different lithofacies types in Lianggaoshan Formation in Well TYX. See Figure 1 for the well location.

10.3389/feart.2022.1032018

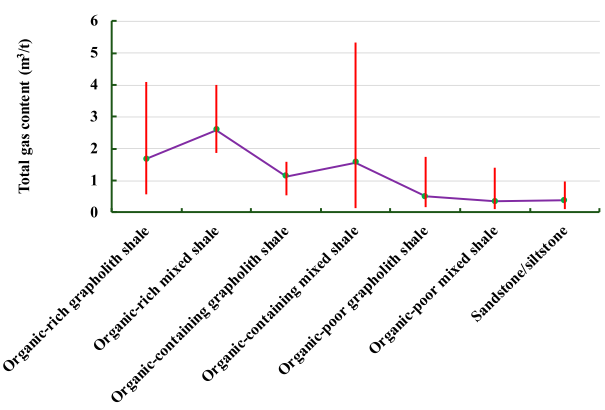

FIGURE 4
Characteristics of gas content in the shale of different lithofacies types in Lianggaoshan Formation in Well TYX. See Figure 1 for the well location.

experiment. Langmuir volume (V_L), with the unit being m^3/t, is the maximum adsorption capacity and physically, it signifies the adsorbed gas content in shale when the adsorption of methane reaches saturation point at a given temperature. Langmuir pressure (P_L), with the unit being MPa, is the pressure at which one-half of the Langmuir volume can be adsorbed.

The isotherm adsorption equation is as follows:

$$V = \frac{V_L P}{P + P_L}$$

Specifically,

V is the maximum adsorption capacity of shale sample under formation pressure P (unit: m^3/t); P is formation pressure (unit: MPa), p=1×9.81×H×formation pressure coefficient/1000, H is burial depth (unit: meter); V_L represents Langmuir volume and P_L Langmuir pressure.

The formation pressure coefficient of the Lianggaoshan Formation in Well TYX is 1.2. The formation pressure can be calculated based on the burial depth of shale samples and the formation pressure coefficient. The maximum adsorbed gas content of the shale samples under formation pressure P can be calculated when the values of P, V_L and P_L are substituted into the isotherm adsorption equation. The calculation results are shown in Table 2. The minimum free gas content can be calculated by subtracting the maximum adsorbed gas content from the measured total gas content, so that the ratio of the maximum adsorbed gas content, as well as the minimum free gas content, to the total gas content in shale can be further calculated. The calculation results are shown in Table 3. According to Table 2 and Table 3, the average value of adsorbed gas content in shale in Well TYX is at most 0.66 m^3/t and the value ranges from 0.06 to 1.06 m^3/t. And adsorbed gas content accounts for at most 40% of the total shale gas content; the average value of free gas content in shale in Well TYX is at least 1.39 m^3/t and the value ranges from 0.09 to 4.39 m^3/t. And free gas content takes up at least 60% of the total shale gas content.

Research on the occurrence space of shale oil and gas

Shale oil and gas occur in the reservoir space of shale matrix, but considering the complex composition and various types of reservoir space of medium-high maturity continental shale, related research is required to find out in what reservoir space the shale oil and gas occur.

TABLE 2 Results of isothermal adsorption experiment and calculation results of formation pressure and maximum adsorbed gas content in Lianggaoshan Formation of Well TYX.

Well depth	Langmuir volume	Langmuir pressure	Formation pressure	Maximum adsorbed gas content
(m)	(m^3/t)	(MPa)	(MPa)	(m^3/t)
2526.95	1.39	19.79	29.75	0.83
2528.74	0.56	6.98	29.77	0.45
2547.26	0.9	10.99	29.99	0.66
2551.36	1.09	9.12	30.03	0.84
2555.56	0.97	10.03	30.08	0.73
2559.1	1.41	10	30.13	1.06
2565.32	0.19	2.81	30.2	0.17
2569.2	1.24	9.24	30.24	0.95
2576.89	1.35	8.88	30.34	1.04
2585.34	0.06	0.88	30.43	0.06

TABLE 3 Ratios of minimum free gas content and maximum adsorbed gas content to total shale gas content and calculation results of minimum free gas content.

Well depth (m)	Maximum adsorbed gas content (m^3/t)	Measured total gas content (m^3/t)	Minimum free gas content (m^3/t)	Ratio of maximum adsorbed gas content (%)	Ratio of minimum free gas content (%)
2526.95	0.83	1.76	0.92	47.53	52.47
2528.74	0.45	0.54	0.09	83.39	16.61
2547.26	0.66	1.86	1.2	35.50	64.50
2551.36	0.84	3.31	2.47	25.28	74.72
2555.56	0.73	4	3.27	18.20	81.80
2559.1	1.06	1.58	0.52	67.09	32.91
2565.32	0.17	0.4	0.22	43.78	56.22
2569.2	0.95	5.34	4.39	17.79	82.21
2576.89	1.04	1.6	0.55	65.39	34.61
2585.34	0.06	0.32	0.26	18.34	81.66

Correlation analyses of shale oil and gas and shale material composition

In order to figure out the occurrence space of shale oil, the S_1 content - TOC content diagram and S_1 content - Clay mineral content diagram are displayed in this study, as shown in Figure 5. There is a fairly positive correlation between S_1 content and TOC content and clay mineral content (Figures 5A,B), which indicates that shale oil mainly occurs in kerogen and clay minerals. S_1 content is largely positively correlated with illite/smectite (I/S) mixed layer and illite (Figures 5C,E), but it is first positively and then negatively correlated with kaolinite and there also exists a slight positive correlation between S_1 content and chlorite (Figures 5D,F), which show that shale oil in clay minerals mainly occurs in I/S mixed layer and illite and only a small amount occurs in kaolinite and chlorite.

In order to figure out the occurrence space of shale gas, this study displays the total gas content - TOC content diagram and total gas content - Clay mineral content diagram, as shown in Figure 6. There is a fairly positive correlation between total gas content and TOC content and clay mineral content (Figures 6A,B), which indicates that shale gas mainly occurs in kerogen and clay minerals. Total gas content is largely positively correlated with illite/smectite (I/S) mixed layer and illite (Figures 6C,E), but it is slightly positively correlated with kaolinite and chlorite (Figures 6D,F), which shows that shale gas in clay minerals mainly occurs in I/S mixed layer and illite and only a small amount occurs in kaolinite and chlorite.

Identification of pore types developed in shale

In order to identify in detail the main pore types developed in shale, the FIB-SEM experiment was performed in this study to observe the organic-rich shale strata in the lower submember of Member II and the upper submember of Member I in the Lianggaoshan Formation. Under the SEM with Ar-ion milling, different material composition of shale manifests different characteristics, among which clay minerals can be easily identified, but the organic macerals with complex classifications are difficult to identify (Hackley and Cardott, 2016; Davudov and Moghanloo, 2018; Davudov et al., 2020). The maceral types in this study are determined through a combination of factors, such as the external form, color, brightness, protrusion of organic matter, the relationship between organic matter and its surrounding minerals, characteristics of organic pore development and fissure development, among others.

As a pretty important organic matter component in shale, solid bitumen is secondary organic matter and is often developed in the mature stage of oil-generating window and gas-generating window (Klaver et al., 2016; Zhang et al., 2017; Zhang et al., 2020b; Zhang et al., 2020c). Solid bitumen-clay mineral complex mass widely exists in such fine-grained sediments as shale. Studies show that in shale, about 72% of the organic matter is bound to clay minerals and they are together preserved in the form of organic clay complex mass. The solid bitumen-clay mineral complex mass has a great influence on the enrichment of oil and gas. Vitrinite is a type of maceral formed by humification and gelation role of lignocellulosic tissues of higher plants. Lignocellulosic structures are often retained in well-preserved vitrinites, in which cell walls and cell lumina are visible, while the badly damaged vitrinites are often granular in all directions and their cell structures are difficult to identify. Vitrinite includes structured vitrinite, unstructured vitrinite, and detrital-vitrinite. Under a polarizing microscope, inertinite reflects white--yellow-white light and this feature distinguishes itself sharply from vitrinite. Inertinite includes fusinite, semi-fusinite and detrital-inertinite (Zou et al., 2019; Wang et al., 2020; Xia et al., 2020; Yu et al., 2022).

As is shown in Figure 7, with the FIB-SEM experiment, the following components were observed: solid bitumen (Figure 7A), solid bitumen-clay mineral complex mass (Figure 7E), clay minerals (Figure 7I), structured vitrinite (Figure 7M), funginite (Figure 7Q), detrital-vitrinite/detrital-inertinite (Figure 7U). Pores are mainly developed in solid bitumen, clay minerals, and solid bitumen-clay mineral complex mass;

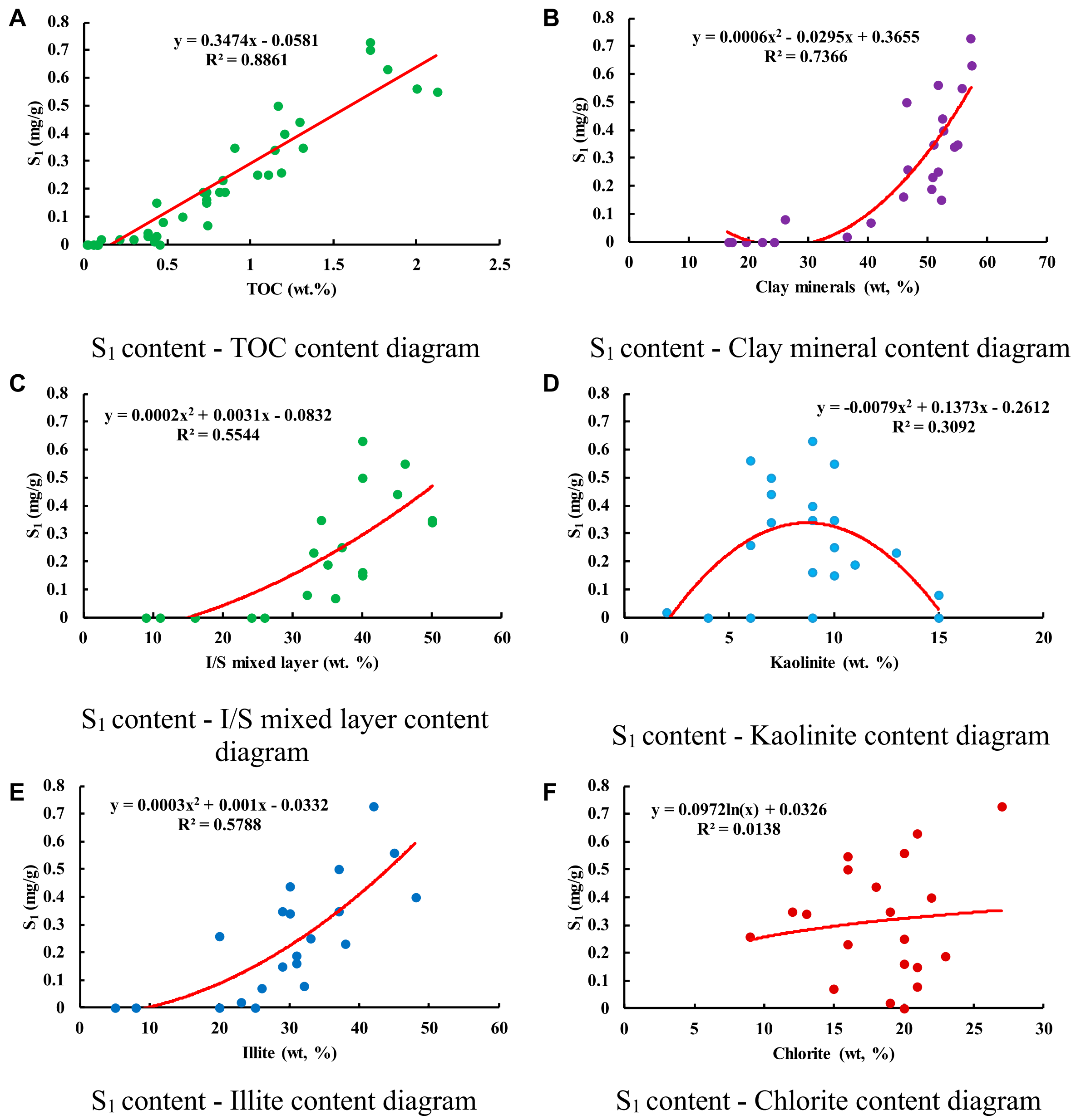

FIGURE 5
Correlation analysis of S_1 content in shale and shale material composition, Lianggaoshan Formation shale in Well TYX. See Figure 1 for the well location.

pores are also partially developed in structured vitrinites and funginite; almost no pores are developed in unstructured vitrinites, vitrinites, fusinite, semi-fusinite and detrital-inertinite.

Quantitative characterization of pore characteristics of shale of different matrices

The software ImageJ is utilized to process images. ImageJ is a Java-based image processing program inspired by USA National Institutes of Health (NIH). Electronic images in TIFF, JPEG, BMP, PNG and other formats can all be processed by ImageJ (Wang et al., 2016a; Wang et al., 2016b; Wang et al., 2017). In the field of oil and gas geology, ImageJ is often used to analyze the pore-fissure structural systems of sedimentary reservoirs. With ImageJ, quantitative characterization of pore development characteristics of specific macerals can be achieved. The imported SEM image which is of high resolution and high

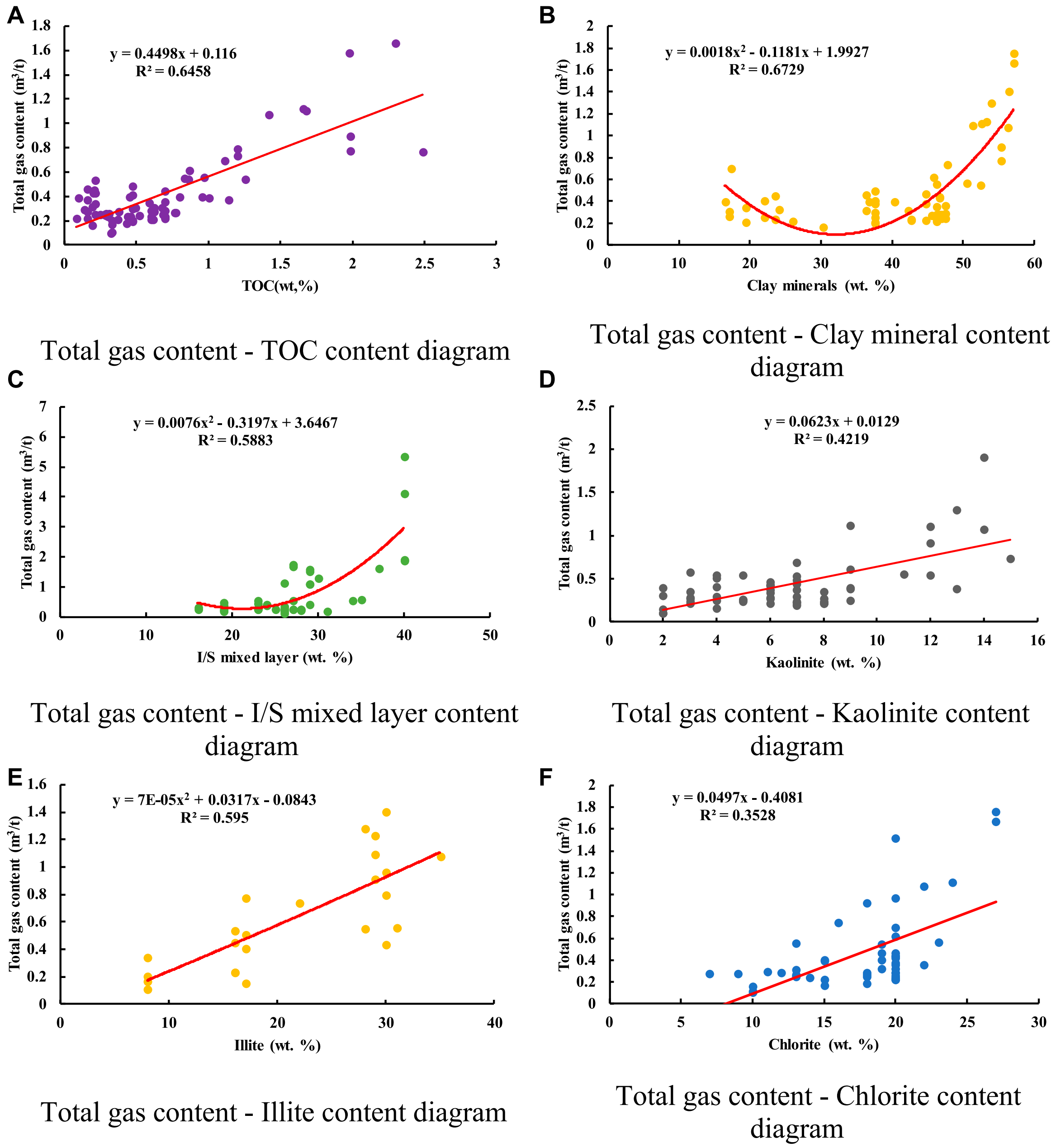

FIGURE 6
Correlation analysis of total gas content in shale and shale material composition, Lianggaoshan Formation shale in Well TYX. See Figure 1 for the well location.

quality was converted to 8bit Gy image and then the organic matter where pores were to be extracted was selected. Since organic matter is generally irregular in shape, the image processing module in ImageJ was used to manually delineate the organic matter. After counting the area of the organic matter, the threshold module in ImageJ was used to segment the pores in the organic matter and the pore area was also counted. The ratio of the pore area to the area of the organic matter is organic pore surface porosity (Zhang et al., 2020a; Zhang et al., 2022a; Zhang et al., 2022b). The final result is the average value of multiple results extracted by different people so as to avoid statistical deviation caused by human factors.

The SEM pictures were processed with ImageJ and the processing procedures are shown in Figure 7. The following pore characteristics of shale of different matrices are secured: perimeter, roundness, average pore diameter, average pore area, number of pores per

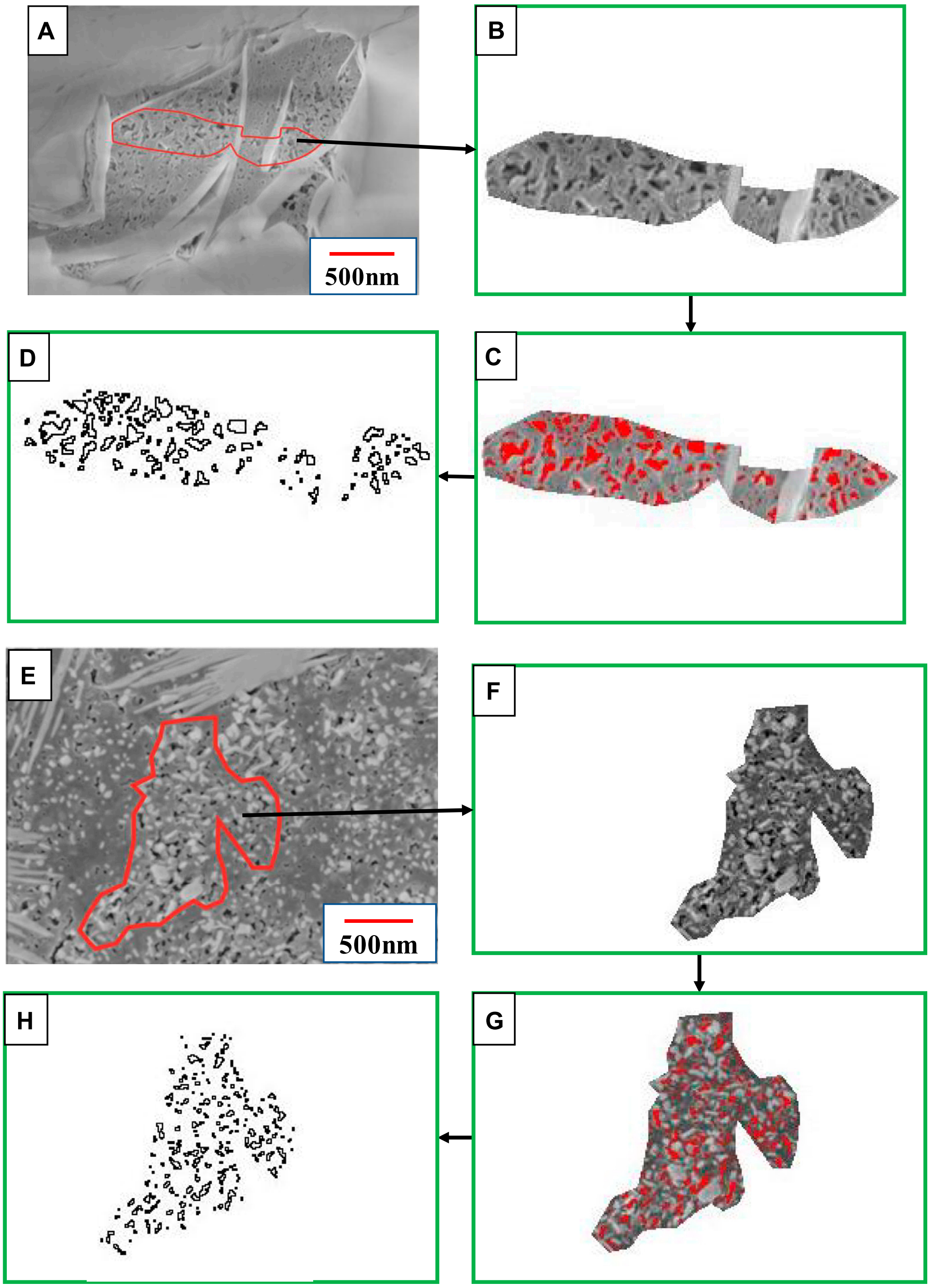

FIGURE 7
Pore types developed in the Lianggaoshan Formation shale in Well TYX and the image processing procedures of ImageJ. Solid bitumen pores and image processing procedures **(A–D)**, 2547.26 m; pores of solid bitumen-clay mineral complex mass and image processing procedures **(E–H)**, 2589.61 m;clay mineral pores and image processing procedures **(I–L)**, 2483.01 m; structured vitrinite pores and image processing procedures **(M–P)**, 2555.56 m; funginite pores and image processing procedures **(Q–T)**, 2547.26 m; detrital-vitrinite/detrital-inertinite pores and image processing procedures **(U–X)**, 2575.25 m. See Figure 1 for the well location.

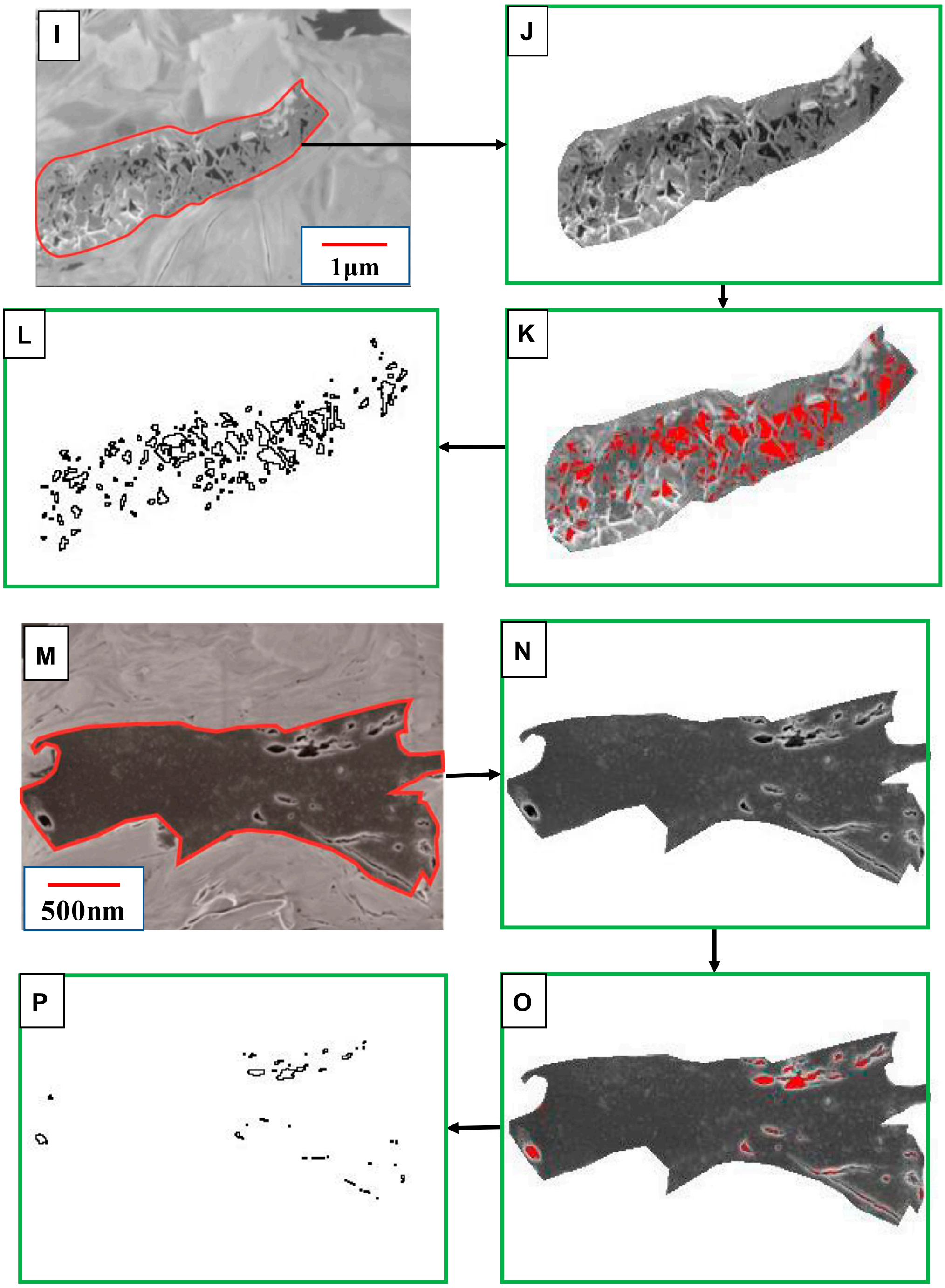

FIGURE 7
(Continued)

unit area, form factor, fractal dimension, average surface porosity, etc. The statistical results of pore characteristics of shale of different matrices are shown in Figure 8, The analyses are as follows: the pores of solid bitumen, solid bitumen-clay mineral complex mass and clay minerals are large in number, with fine roundness, medium pore diameter, fairly good roundness of pore edges and complex shapes, thus altogether contributing to their large surface porosity, i.e., 17.791, 11.147 and 12.991%, respectively. Therefore, these pores are the main reservoir space of shale oil and gas. Funginite pores have medium pore diameter, good roundness, average number, good roundness of

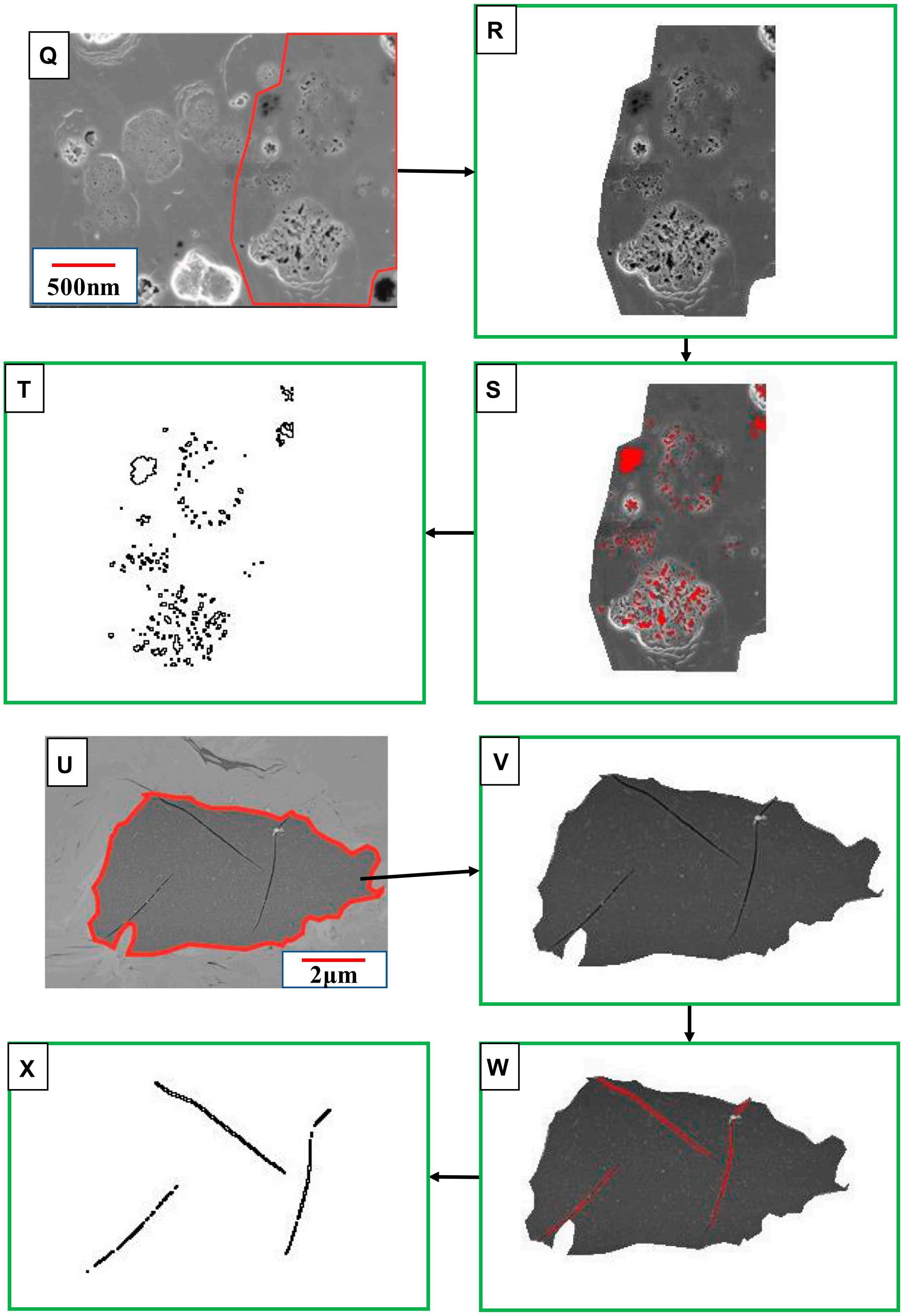

FIGURE 7
(Continued)

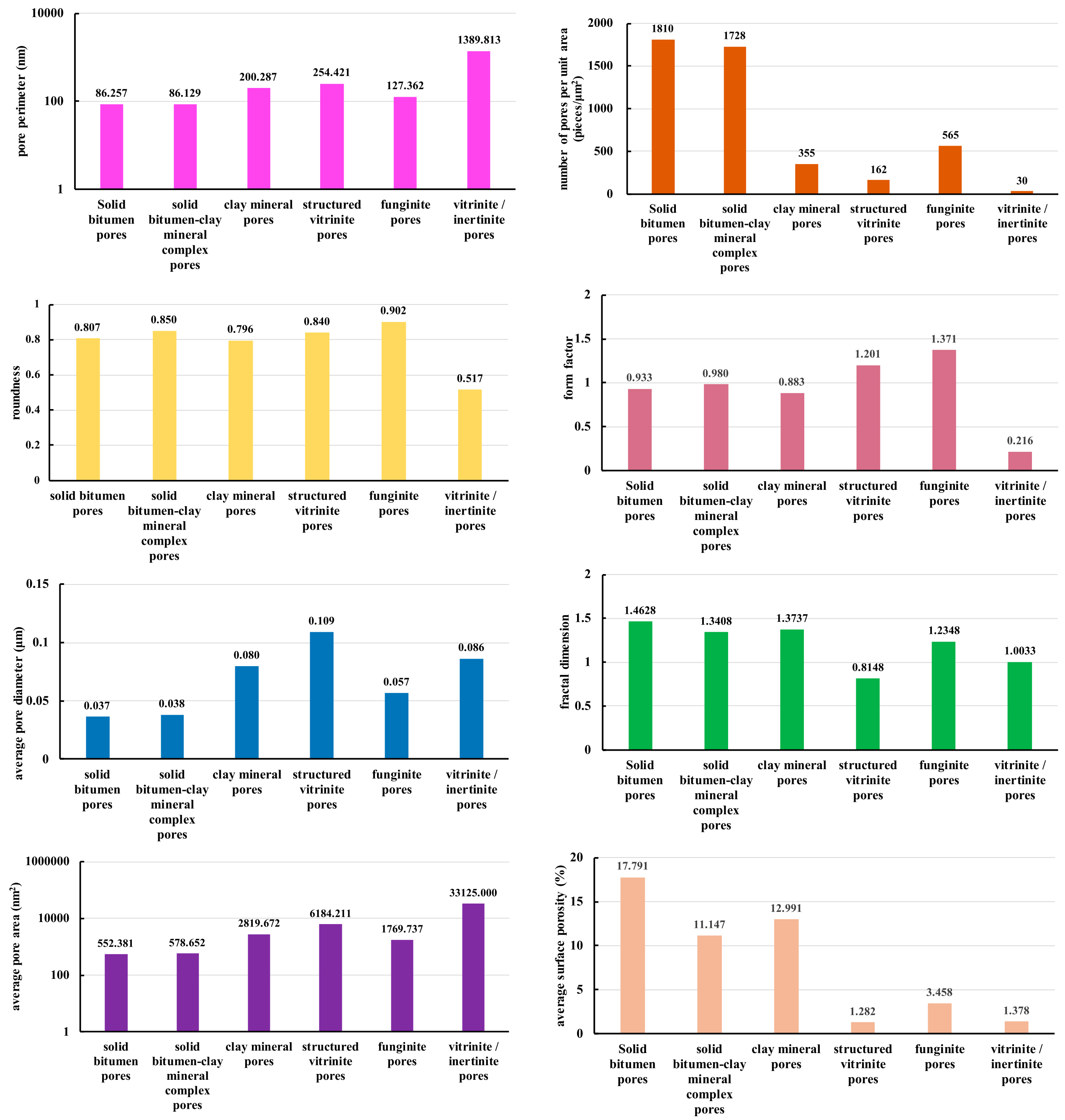

FIGURE 8
Quantitative characterization of pore characteristics of shale with different matrices in Lianggaoshan Formation in Well TYX. See Figure 1 for the well location.

pore edges, and relatively complex shapes, which altogether lead to its medium surface porosity of 3.458%. Funginite pores partially serve as the reservoir space of shale oil and gas. Small in number, structured vitrinite pores have good roundness, large pore diameter, good roundness of pore edges, and relatively complex shapes, which altogether result in the low surface porosity of 1.282%. Structured vitrinite pores slightly function as the reservoir space of shale oil and gas. Small in number, the pores of detrital-vitrinite/detrital-inertinite and the microfractures developed in them have large pore diameters, poor roundness, poor roundness of pore edges, and relatively complex shapes, thus resulting in the low surface porosity of 1.378%. Hence, these pores slightly work as the reservoir space of shale oil and gas.

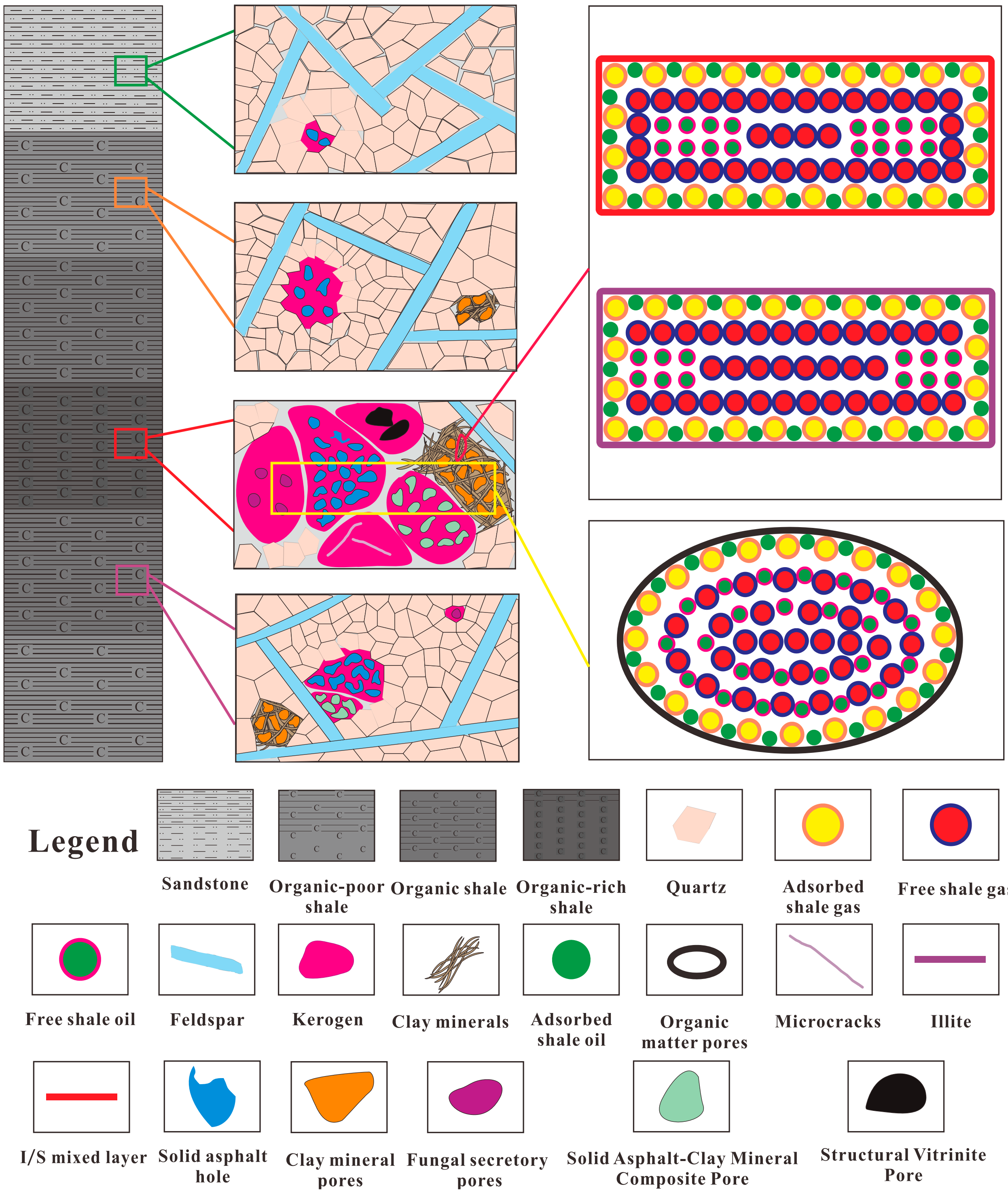

FIGURE 9
Summary of patterns of pore characteristic of medium-high maturity continental shale oil and gas occurrence.

Summary of patterns of pore characteristics of shale oil and gas occurrence

After the above discussion, the patterns of pore characteristics of shale oil and gas occurrence are summarized, which is shown in Figure 9. In terms of lithofacies, medium-high maturity continental shale oil and gas mainly occur in organic-rich clayey shale and organic-rich mixed shale. With regard to the material composition, shale oil and gas mainly occur in clay minerals including organic matter, illite-smectite mixed layers and illite. As for pore types, shale oil and gas mainly occur in the pores of solid bitumen, solid bitumen-clay mineral complex mass and clay minerals, and partly occur in structured vitrinite pores and funginite pores. Among them, pores of solid bitumen, structured vitrinites and funginite are organic.

Conclusion

Focused on shale from the Middle Jurassic Lianggaoshan Formation in Well TYX, Fuling block, southeast of Sichuan Basin in the Upper Yangtze region of southern China, this study, selecting shale core samples, has conducted a series of analyses and they are: vitrinite reflectance analysis and kerogen microscopic examination experiment, the identification of shale organic geochemical characteristics, TOC content analysis and mineral composition analysis, the classification of shale lithofacies, S_1 content analysis, gas content measurement and isothermal adsorption experiment, the identification of oil-gas-bearing potential of shale of different lithofacies, as well as occurrence space of shale oil and gas. The SEM with Ar-ion milling and ImageJ were used to identify the main pore types developed in shale, and the pore characteristics of shale of different matrices were quantitatively characterized. The conclusions are drawn as follows:

1) In terms of lithofacies, medium-high maturity continental shale oil and gas mainly occur in organic-rich clayey shale and organic-rich mixed shale.
2) With regard to the material composition, shale oil and gas mainly occur in organic matter, illite-smectite mixed layers and illite which are of clay minerals. The adsorbed gas content in shale accounts for at most 40% of the total shale gas content and the free gas content in shale takes up at least 60% of the total shale gas content.
3) As for pore types, shale oil and gas mainly occur in the pores of solid bitumen, solid bitumen-clay mineral complex mass and clay minerals, and partly occur in structured vitrinite pores and funginite pores.
4) Large in number, the pores of solid bitumen, solid bitumen-clay mineral complex mass, and clay minerals, with the characteristics of fine roundness and large surface porosity, are the main reservoir space of shale oil and gas; funginite pores, with medium pore diameter, good roundness and medium surface porosity, partially serve as the reservoir space of shale oil and gas; small in number, structured vitrinite pores, with good roundness and low surface porosity, slightly function as the reservoir space of shale oil and gas; the pores of detrital-vitrinite/detrital-inertinite and the microfractures developed in them have large pore diameters, poor roundness and low surface porosity, so the pores are merely the reservoir space of shale oil and gas.

Data availability statement

The raw data supporting the conclusions of this article will be made available by the authors, without undue reservation.

Author contributions

XY, KZ, and JP contributed to the conception and design of the study. BL organized the database. FH performed the statistical analysis. XY, KZ, and JP wrote the first draft of the manuscript. XC, ZZ, JR, LY, ZW, ZH, KC, MW, JN, and ZY wrote the sections of the manuscript. All authors contributed to manuscript revision, read, and approved the submitted version.

Funding

This study was supported by the open funds from the National Natural Science Foundation of China (42102192, 42130803 and 42072174), the Open Fund of Key Laboratory of Tectonics and Petroleum Resources (China University of Geosciences), Ministry of Education, Wuhan (TPR-2022-08), the open experiment fund of Southwest Petroleum University (2021KSP02029), the Tianfu Emei Project Youth Talent Project (1963), and the Science and Technology Cooperation Project of the CNPC-SWPU Innovation Alliance.

Acknowledgments

We sincerely appreciate all reviewers and the handling editor for their critical comments and constructive suggestions.

Conflict of interest

The authors declare that the research was conducted in the absence of any commercial or financial relationships that could be construed as a potential conflict of interest.

Publisher's note

All claims expressed in this article are solely those of the authors and do not necessarily represent those of their affiliated organizations, or those of the publisher, the editors and the reviewers. Any product that may be evaluated in this article, or claim that may be made by its manufacturer, is not guaranteed or endorsed by the publisher.

References

Adeleye, J., and Akanji, L. (2018). Pore-scale analyses of heterogeneity and representative elementary volume for unconventional shale rocks using statistical tools. *J. Pet. Explor. Prod. Technol.* 8 (3), 753–765. doi:10.1007/s13202-017-0377-4

Ardakani, O., Sanei, H., Ghanizadeh, A., Lavoie, D., Chen, Z., and Clarkson, C. R. (2018). Do all fractions of organic matter contribute equally in shale porosity? A case study from upper ordovician utica shale, southern quebec, Canada. *Mar. Petroleum Geol.* 92, 794–808. doi:10.1016/j.marpetgeo.2017.12.009

Bakshi, T., and Vishal, V. (2021). A review on the role of organic matter in gas adsorption in shale. *Energy fuels.* 35 (19), 15249–15264. doi:10.1021/acs.energyfuels.1c01631

Bazilian, M., Brandt, A., Billman, L., Heath, G., Logan, J., Mann, M., et al. (2014). Ensuring benefits from North American shale gas development: Towards a research agenda. *J. Unconv. Oil Gas Resour.* 7, 71–74. doi:10.1016/j.juogr.2014.01.003

Clarkson, C., Solano, N., Bustin, R., Bustin, A., Chalmers, G., He, L., et al. (2013). Pore structure characterization of North American shale gas reservoirs using USANS/SANS, gas adsorption, and mercury intrusion. *Fuel* 103, 606–616. doi:10.1016/j.fuel.2012.06.119

Daigle, H., Hayman, N., Kelly, E., Milliken, K., and Jiang, H. (2017). Fracture capture of organic pores in shales. *Geophys. Res. Lett.* 44 (5), 2167–2176. doi:10.1002/2016gl072165

Davudov, D., and Moghanloo, R. (2018). Impact of pore compressibility and connectivity loss on shale permeability. *Int. J. Coal Geol.* 187, 98–113. doi:10.1016/j.coal.2018.01.008

Davudov, D., Moghanloo, R., and Zhang, Y. (2020). Interplay between pore connectivity and permeability in shale sample. *Int. J. Coal Geol.* 220, 103427. doi:10.1016/j.coal.2020.103427

Fan, C., Xie, H., Li, H., Zhao, S., Shi, X., Liu, J., et al. (2022). Complicated fault characterization and its influence on shale gas preservation in the southern margin of the Sichuan Basin, China. *Lithosphere* 2022, 8035106. doi:10.2113/2022/8035106

Gao, F. (2021). Influence of hydraulic fracturing of strong roof on mining-induced stress insight from numerical simulation. *J. Min. Strata Control Eng.* 3 (2), 023032. doi:10.13532/j.jmsce.cn10-1638/td.20210329.001

Gao, J., Wang, X., He, S., Guo, X., Zhang, B., and Chen, X. (2017). Geochemical characteristics and source correlation of natural gas in Jurassic shales in the North Fuling area, Eastern Sichuan Basin, China. *J. Petroleum Sci. Eng.* 158, 284–292. doi:10.1016/j.petrol.2017.08.055

Gao, Z., Fan, Y., Hu, Q., Jiang, Z., and Cheng, Y. (2020). The effects of pore structure on wettability and methane adsorption capability of Longmaxi Formation shale from the southern Sichuan Basin in China. *Am. Assoc. Pet. Geol. Bull.* 104 (6), 1375–1399. doi:10.1306/01222019079

Gao, Z., Hu, Q., and Hamamoto, S. (2018). Using multicycle mercury intrusion porosimetry to investigate hysteresis phenomenon of different porous media. *J. Porous Media* 21 (7), 607–622. doi:10.1615/jpormedia.2018017822

Guo, T. (2016). Key geological issues and main controls on accumulation and enrichment of Chinese shale gas. *Petroleum Explor. Dev.* 43 (3), 349–359. (in Chinese with English abstract). doi:10.1016/s1876-3804(16)30042-8

Guo, X., Hu, D., Li, Y., Wei, Z., Wei, X., and Liu, Z. (2017). Geological factors controlling shale gas enrichment and high production in Fuling shale gas field. *Petroleum Explor. Dev.* 44 (4), 513–523. (in Chinese with English abstract). doi:10.1016/s1876-3804(17)30060-5

Guo, X., Hu, D., Wei, Z., et al. (2016). Discovery and exploration of Fuling shale gas field. *China Pet. Explor.* 21 (3), 24. doi:10.3969/j.issn.1672-7703.2016.03.003

Hackley, P., and Cardott, B. (2016). Application of organic petrography in North American shale petroleum systems: A review. *Int. J. Coal Geol.* 163, 8–51. doi:10.1016/j.coal.2016.06.010

He, Z., Li, S., Nie, H., Yuan, Y., and Wang, H. (2019). The shale gas "sweet window": "The cracked and unbroken" state of shale and its depth range. *Mar. Petroleum Geol.* 101, 334–342. doi:10.1016/j.marpetgeo.2018.11.033

He, Z., Nie, H., Li, S., Luo, J., Wang, H., and Zhang, G. (2020). Differential enrichment of shale gas in upper Ordovician and lower Silurian controlled by the plate tectonics of the Middle-Upper Yangtze, south China. *Mar. Petroleum Geol.* 118, 104357. doi:10.1016/j.marpetgeo.2020.104357

Jiang, Z., Li, T., Gong, H., et al. (2020). Characteristics of low-mature shale reservoirs in Zhanhua Sag and their influence on the mobility of shale oil. *Acta Pet. Sin.* 41 (12), 1587. doi:10.7623/syxb202012011

Jin, Z., Nie, H., Liu, Q., Zhao, J., and Jiang, T. (2018). Source and seal coupling mechanism for shale gas enrichment in upper ordovician wufeng formation-lower silurian Longmaxi Formation in Sichuan Basin and its periphery. *Mar. Petroleum Geol.* 97, 78–93. doi:10.1016/j.marpetgeo.2018.06.009

Jin, Z., Nie, H., Liu, Q., Zhao, J., Wang, R., Sun, C., et al. (2020). Coevolutionary dynamics of organic-inorganic interactions, hydrocarbon generation, and shale gas reservoir preservation: A case study from the upper ordovician wufeng and lower silurian longmaxi formations, fuling shale gas field, eastern Sichuan Basin. *Geofluids*, 1–21. doi:10.1155/2020/6672386

Klaver, J., Desbois, G., Littke, R., and Urai, J. (2016). BIB-SEM pore characterization of mature and post mature Posidonia Shale samples from the Hils area, Germany. *Int. J. Coal Geol.* 158, 78–89. doi:10.1016/j.coal.2016.03.003

Li, C., He, D., Lu, G., Wen, K., Simon, A., and Sun, Y. (2021a). Multiple thrust detachments and their implications for hydrocarbon accumulation in the northeastern Sichuan Basin, southwestern China. *Am. Assoc. Pet. Geol. Bull.* 105 (2), 357–390. doi:10.1306/07272019064

Li, D., Li, J., Zhang, B., Yang, J., and Wang, S. (2017). Formation characteristics and resource potential of Jurassic tight oil in Sichuan Basin. *Petroleum Res.* 2 (4), 301–314. doi:10.1016/j.ptlrs.2017.05.001

Li, H., Qin, Q., Zhang, B., Ge, X., Hu, X., Fan, C., et al. (2020a). Tectonic fracture formation and distribution in ultradeep marine carbonate gas reservoirs: A case study of the maokou Formation in the jiulongshan gas field, Sichuan Basin, southwest China. *Energy fuels.* 34 (11), 14132–14146. doi:10.1021/acs.energyfuels.0c03327

Li, H. (2022). Research progress on evaluation methods and factors influencing shale brittleness: A review. *Energy Rep.* 8, 4344–4358. doi:10.1016/j.egyr.2022.03.120

Li, H., Tang, H., Qin, Q., Zhou, J., Qin, Z., Fan, C., et al. (2019). Characteristics, formation periods and genetic mechanisms of tectonic fractures in the tight gas sandstones reservoir: A case study of xujiahe Formation in YB area, Sichuan Basin, China. *J. Petroleum Sci. Eng.* 178, 723–735. doi:10.1016/j.petrol.2019.04.007

Li, J., Li, H., Yang, C., et al. (2022a). *Geological characteristics and controlling factors of deep shale gas enrichment of the Wufeng-Longmaxi Formation in the southern Sichuan Basin*. China: Lithosphere, 4737801.

Li, J., Tao, S., and Wang, Z. (2010). Characteristics of Jurassic petroleum geology and main factors of hydrocarbon accumulation in NE Sichuan basin. *Nat. Gas. Geosci.* 21 (5), 732–741.

Li, X., Jiang, Z., Jiang, S., Li, Z., Song, Y., Jiang, H., et al. (2020b). Characteristics of matrix-related pores associated with various lithofacies of marine shales inside of Guizhong Basin, South China. *J. Pet. Sci. Eng.* 185, 106671. doi:10.1016/j.petrol.2019.106671

Li, X., Jiang, Z., Jiang, S., Li, Z., Song, Y., Jiang, H., et al. (2020c). Various controlling factors of matrix-related pores from differing depositional shales of the yangtze block in south China: Insight from organic matter isolation and fractal analysis. *Mar. Pet. Geol.* 111, 720–734. doi:10.1016/j.marpetgeo.2019.08.019

Li, X., Jiang, Z., Jiang, S., Wang, S., Miao, Y., Cao, X., et al. (2021b). Synergetic effects of matrix components and diagenetic processes on pore properties in the lower cambrian shale in sichuan basin, south China. *J. Nat. Gas. Sci. Eng.* 94 (4-5), 104072. doi:10.1016/j.jngse.2021.104072

Li, X., Jiang, Z., Wang, S., Wu, F., Miao, Y., Wang, X., et al. (2022b). Differences of marine and transitional shales in the case of dominant pore types and exploration strategies, in China. *J. Nat. Gas. Sci. Eng.* 103, 104628. doi:10.1016/j.jngse.2022.104628

Li, X., Wang, P., Wang, S., Can, J., Zhang, C., Zhao, R., et al. (2021c). Influence of the duration of tectonic evolution on organic matter pore structure and gas enrichment in marine shale: A case study of the lower silurian longmaxi shale in southern China. *Front. Earth Sci. (Lausanne).* 9, 787697. doi:10.3389/feart.2021.787697

Liu, B., He, S., Meng, L., Fu, X., Gong, L., and Wang, H. (2021b). Sealing mechanisms in volcanic faulted reservoirs in xujiaweizi extension, northern songliao basin, northeastern China. *Am. Assoc. Pet. Geol. Bull.* 2021 (20315), 1721–1743. doi:10.1306/03122119048

Liu, B., Sun, J., Zhang, Y., He, J., Fu, X., Yang, L., et al. (2021c). Reservoir space and enrichment model of shale oil in the first member of Cretaceous Qingshankou Formation in the Changling sag, southern Songliao Basin, NE China. *Petroleum Explor. Dev.* 48 (3), 608–624. doi:10.1016/s1876-3804(21)60049-6

Liu, W., Zhang, K., Li, Q., Yu, Z., Cheng, S., Liu, J., et al. (2021a). Quantitative characterization for the micronanopore structures of terrestrial shales with different lithofacies types: A case study of the jurassic Lianggaoshan Formation in the southeastern Sichuan Basin of the yangtze region. *Geofluidsuids* 2021, 1–16. doi:10.1155/2021/1416303

Liu, Z., Liu, G., Hu, Z., Feng, D., Zhu, T., Bian, R., et al. (2020). Lithofacies types and assemblage features of continental shale strata and their implications for shale gas exploration: A case study of the middle and lower jurassic strata in the Sichuan Basin. *Nat. Gas. Ind. B* 7 (4), 358–369. doi:10.1016/j.ngib.2019.12.004

Liu, Z., and Ni, C. (2010). Characteristics of sandstone reservoirs of middle-lower Jurassic in central Sichuan Area. *J. Southwest Petroleum Univ. Sci. Technol. Ed.* 32 (2), 35. doi:10.3863/j.issn.1674-5086.2010.02.007

Loucks, R., Ruppel, S., Wang, X., Ko, L., Peng, S., Zhang, T., et al. (2017). Pore types, pore-network analysis, and pore quantification of the lacustrine shale-hydrocarbon system in the Late Triassic Yanchang Formation in the southeastern Ordos Basin, China. *Interpretation* 5 (2), SF63–SF79. doi:10.1190/int-2016-0094.1

Nie, H., Sun, C., Liu, G., Du, W., and He, Z. (2019). Dissolution pore types of the wufeng formation and the Longmaxi Formation in the Sichuan Basin, south China: Implications for shale gas enrichment. *Mar. Petroleum Geol.* 101, 243–251. doi:10.1016/j.marpetgeo.2018.11.042

Pang, Z., Tao, S., Zhang, Q., Zhang, T., Yang, J., Fan, J., et al. (2019). Enrichment factors and sweep spot evaluation of Jurassic tight oil in central Sichuan Basin, SW China. *Petroleum Res.* 4 (4), 334–347. doi:10.1016/j.ptlrs.2019.05.001

Qing, Y., Lü, Z., Wu, J., Yang, J. J., Zhang, S. L., Xiong, C. H., et al. (2019). Formation mechanisms of calcite cements in tight sandstones of the jurassic Lianggaoshan Formation, northeastern central Sichuan Basin. *Aust. J. Earth Sci.* 66 (5), 723–740. doi:10.1080/08120099.2018.1564935

Wang, J., Zhang, C., Zheng, D., et al. (2020). Stability analysis of roof in goaf considering time effect. *J. Min. Strata Control Eng.* 2 (1), 013011. doi:10.13532/j.jmsce.cn10-1638/td.2020.01.005

Wang, P., Jiang, Z., Chen, L., Yin, L., Li, Z., Zhang, C., et al. (2016a). Pore structure characterization for the longmaxi and niutitang shales in the upper yangtze platform, south China: Evidence from focused ion beam-He ion microscopy, nano-computerized tomography and gas adsorption analysis. *Mar. Petroleum Geol.* 77, 1323–1337. doi:10.1016/j.marpetgeo.2016.09.001

Wang, P., Jiang, Z., Ji, W., Zhang, C., Yuan, Y., Chen, L., et al. (2016b). Heterogeneity of intergranular, intraparticle and organic pores in longmaxi shale in Sichuan Basin, south China: Evidence from SEM digital images and fractal and multifractal geometries. *Mar. Petroleum Geol.* 72, 122–138. doi:10.1016/j.marpetgeo.2016.01.020

Wang, P., Jiang, Z., Yin, L., Chen, L., Li, Z., Zhang, C., et al. (2017). Lithofacies classification and its effect on pore structure of the Cambrian marine shale in the Upper Yangtze Platform, South China: Evidence from FE-SEM and gas adsorption analysis. *J. Petroleum Sci. Eng.* 156, 307–321. doi:10.1016/j.petrol.2017.06.011

Wang, R., Hu, Z., Long, S., Liu, G., Zhao, J., Dong, L., et al. (2019). Differential characteristics of the upper ordovician-lower silurian wufeng-longmaxi shale reservoir and its implications for exploration and development of shale gas in/around the sichuan basin. *Acta Geol. sinica-. Engl. Ed.* 93 (3), 520–535. doi:10.1111/1755-6724.13875

Wang, X., He, S., Guo, X., Zhang, B., and Chen, X. (2018). The resource evaluation of Jurassic shale in North Fuling area, eastern Sichuan Basin, China. *Energy fuels.* 32 (2), 1213–1222. doi:10.1021/acs.energyfuels.7b03097

Wang, Z., Wang, J., Yu, F., Fu, X., Chen, W., Zhan, W., et al. (2021a). Geochemical characteristics of the Upper Triassic black mudstones in the eastern Qiangtang Basin, Tibet: Implications for petroleum potential and depositional environment. *J. Petroleum Sci. Eng.* 2021207, 109180. doi:10.1016/j.petrol.2021.109180

Wang, Z., Yu, F., Wang, J., Fu, X., Chen, W., Zeng, S., et al. (2021b). Palaeoenvironment evolution and organic matter accumulation of the Upper Triassic mudstones from the eastern Qiangtang Basin (Tibet), eastern Tethys. *Mar. Petroleum Geol.* 130, 105113. doi:10.1016/j.marpetgeo.2021.105113

Wang, L, L., Ye, Y., Qin, J., et al. (2022). Microscopic pore structure characterization and oil-bearing property evaluation of lacustrine shale reservoir:A case study of the Permian Lucaogou Formation in Jimsar Sag, Junggar Basin. *Oil Gas Geol.* 43 (1), 149–160. doi:10.11743/ogg20220112 (in Chinese with English abstract).

Wang, Z, Z., Shen, L., Wang, J., Fu, X., Xiao, Y., Song, C., et al. (2022). Organic matter enrichment of the late triassic bagong formation (qiangtang basin, tibet) driven by paleoenvironment: Insights from elemental geochemistry and mineralogy. *J. Asian Earth Sci.* 236, 105329. doi:10.1016/j.jseaes.2022.105329

Wei, X., Zhang, K., Li, Q., Hu, D., Wei, Z., Liu, R., et al. (2021). Quantitative characterization of pore space for the occurrence of continental shale oil in lithofacies of different types: Middle Jurassic Lianggaoshan Formation in southeastern Sichuan Basin of the upper Yangtze area. *Geofluids* 2021, 1–18. doi:10.1155/2021/9906500

Xia, Y., Lu, C., Yang, G., et al. (2020). Experimental study on axial fracture cutting and fracturing of abrasive jet in hard roof hole. *J. Min. Strata Control Eng.* 2 (3), 033522.

Yu, X., Bian, J., and Liu, C. (2022). Determination of energy release parameters of hydraulic fracturing roof near goaf based on surrounding rock control of dynamic pressure roadway. *J. Min. Strata Control Eng.* 4 (1), 013016. doi:10.13532/j.jmsce.cn10-1638/td.20210908.001

Zhang, K., Jia, C., Song, Y., Jiang, S., Jiang, Z., Wen, M., et al. (2020a). Analysis of lower cambrian shale gas composition, source and accumulation pattern in different tectonic backgrounds: A case study of weiyuan block in the upper yangtze region and xiuwu Basin in the lower yangtze region. *Fuel* 263 (2020), 115978. doi:10.1016/j.fuel.2019.115978

Zhang, K., Jiang, S., Zhao, R., Wang, P., Jia, C., and Song, Y. (2022a). Connectivity of organic matter pores in the Lower silurian longmaxi formation shale, sichuan basin, southern China: Analyses from helium ion microscope and focused ion beam scanning electron microscope. *Geol. J.* 57, 1912–1924. doi:10.1002/gj.4387

Zhang, K., Jiang, Z., Song, Y., Jia, C., Yuan, X., Wang, X., et al. (2022b). Quantitative characterization for pore connectivity, pore wettability, and shale oil mobility of terrestrial shale with different lithofacies -- A case study of the Jurassic Lianggaoshan Formation in the Southeast Sichuan Basin of the Upper Yangtze Region in Southern China. *Front. Earth Sci. (Lausanne).* 2022, 864189. doi:10.3389/feart.2022.864189

Zhang, K., Jiang, Z., Yin, L., Gao, Z., Wang, P., Song, Y., et al. (2017). Controlling functions of hydrothermal activity to shale gas content-taking lower cambrian in Xiuwu Basin as an example. *Mar. Petroleum Geol.* 85, 177–193. doi:10.1016/j.marpetgeo.2017.05.012

Zhang, K., Peng, J., Liu, W., Li, B., Xia, Q., Cheng, S., et al. (2020b). The role of deep geofluids in the enrichment of sedimentary organic matter: A case study of the late ordovician-early silurian in the upper yangtze region and early cambrian in the lower yangtze region, south China. *Geofluids* 2020, 1–12. doi:10.1155/2020/8868638

Zhang, K., Peng, J., Wang, X., Jiang, Z., Song, Y., Jiang, L., et al. (2020c). Effect of organic maturity on shale gas Genesis and pores development: A case study on marine shale in the upper yangtze region, south China. *Open Geosci.* 12 (2020), 1617–1629. doi:10.1515/geo-2020-0216

Zhang, K., Song, Y., Jia, C., Jiang, Z., Han, F., Wang, P., et al. (2022c). Formation mechanism of the sealing capacity of the roof and floor strata of marine organic-rich shale and shale itself, and its influence on the characteristics of shale gas and organic matter pore development. *Mar. Petroleum Geol.* 140 (2022), 105647. doi:10.1016/j.marpetgeo.2022.105647

Zhang, K., Song, Y., Jia, C., Jiang, Z., Jiang, S., Huang, Y., et al. (2019a). Vertical sealing mechanism of shale and its roof and floor and effect on shale gas accumulation, a case study of marine shale in Sichuan basin, the Upper Yangtze area. *J. Petroleum Sci. Eng.* 175, 743–754. doi:10.1016/j.petrol.2019.01.009

Zhang, K., Song, Y., Jiang, S., Jiang, Z., Jia, C., Huang, Y., et al. (2019b). Mechanism analysis of organic matter enrichment in different sedimentary backgrounds: A case study of the lower cambrian and the upper ordovician-lower silurian, in yangtze region. *Mar. Petroleum Geol.* 99, 488–497. doi:10.1016/j.marpetgeo.2018.10.044

Zhang, K., Song, Y., Jiang, S., Jiang, Z., Jia, C., Huang, Y., et al. (2019c). Shale gas accumulation mechanism in a syncline setting based on multiple geological factors: An example of southern Sichuan and the Xiuwu Basin in the Yangtze Region. *Fuel* 241, 468–476. doi:10.1016/j.fuel.2018.12.060

Zhang, K., Song, Y., Jiang, Z., Xu, D., Li, L., Yuan, X., et al. (2022d). Quantitative comparison of Genesis and pore structure characteristics of siliceous minerals in marine shale with different TOC contents - a case study on the shale of Lower Silurian Longmaxi Formation in Sichuan Basin, Southern China. *Front. Earth Sci. (Lausanne).* 2022, 887160. doi:10.3389/feart.2022.887160

Zhang, K., Song, Y., Jiang, Z., Yuan, X., Wang, X., Han, F., et al. (2022e). Research on the occurrence state of methane molecules in post-mature marine shales-A case analysis of the Lower Silurian Longmaxi Formation shales of the upper Yangtze region in Southern China. *Front. Earth Sci. (Lausanne).* 2022, 864279. doi:10.3389/feart.2022.864279

Zhang, S., Liu, H., Wang, M., et al. (2018). Pore evolution of shale oil reservoirs in Dongying Sag. *Acta Pet. Sin.* 39 (7), 754–766. doi:10.7623/syxb201807003 (in Chinese with English abstract).

Zuo, J., Yu, M., Hu, S., et al. (2019). Experimental investigation on fracture mode of different thick rock strata. *J. Min. Strata Control Eng.* 1 (1), 013007. doi:10.13532/j.jmsce.cn10-1638/td.2019.02.008